Scientific and Engineering Applications of Lasers

Trudy Bellinger

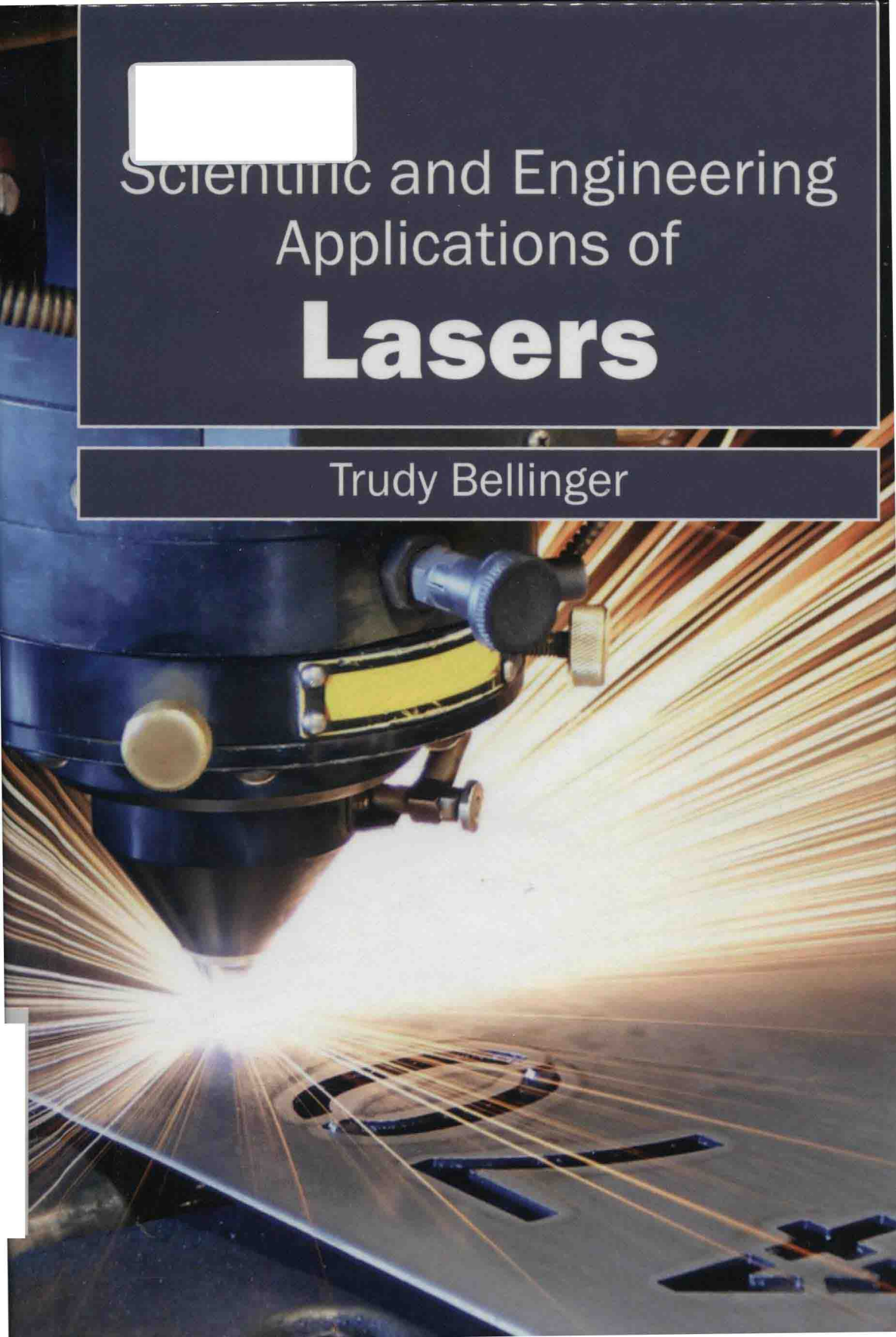

Scientific and Engineering Applications of Lasers

Edited by **Trudy Bellinger**

CLANRYE INTERNATIONAL

New Jersey

Published by Clanrye International,
55 Van Reypen Street,
Jersey City, NJ 07306, USA
www.clanryeinternational.com

Scientific and Engineering Applications of Lasers
Edited by Trudy Bellinger

International Standard Book Number: 978-1-63240-458-9 (Hardback)

Printed in the United States of America.

Scientific and Engineering Applications of Lasers

Preface

This book provides an extensive analysis of lasers and their applications. The book begins with a general analysis of physical phenomena on laser-matter interplay, followed by description of several laser applications in materials evaluation for industry, biological applications (in-vitro fertilization, tissue ablation), nano-particles and thin films production, and long-range detection issues by LIDARs.

This book is the end result of constructive efforts and intensive research done by experts in this field. The aim of this book is to enlighten the readers with recent information in this area of research. The information provided in this profound book would serve as a valuable reference to students and researchers in this field.

At the end, I would like to thank all the authors for devoting their precious time and providing their valuable contribution to this book. I would also like to express my gratitude to my fellow colleagues who encouraged me throughout the process.

Editor

Contents

Part 1

Thin Films and Nanostructures

1

Laser Pulse Patterning on Phase Change Thin Films

Jingsong Wei[1] and Mufei Xiao[2]
[1]*Shanghai Institute of Optics and Fine Mechanics, Chinese Academy of Sciences*
[2]*Centro de Nanociencias y Nanotecnología, Universidad Nacional Autónoma de México*
[1]*China*
[2]*México*

1. Introduction

In the present chapter, we discuss the formation of microscopic patterns on phase change thin films with low power laser pulses. The discussions are mostly based on our recent experimental and theoretical results on the subject.

Phase change thin films are widely used as optical and electric data storage media. The recording is based on the phase change between the crystalline and amorphous states. In the writing process, a small volume in the thin film is locally and rapidly heated to above the melting point and successively quenched into the amorphous phase. In the erasing process, the material undergoes a relatively long heating to reach a temperature above the glass transition but yet below the melting point, which brings the material back to the crystalline phase.

However, during the writing process, apart from the phase changes, physical deformation of the surface occurs, which often creates bumps of various forms. In other words, low intensity laser pulses are able to microscopically form patterns on phase change films. The formed patterns modify the topographic landscape of the surface and bring about variations on the material properties of the films. The modifications can be harmful or helpful depending on what kind of applications one looks for. Therefore, in order to properly deal with the laser induced bumps, it is essential to understand the process of bump formation, and to qualitatively and quantitatively describe the created bumps as well as its relation with the laser pulse parameters, such as the beam distributions and the average intensity etc. so that one is able to closely control the formation of microscopic patterns on phase change films with low power laser pulses. Recently, we have systematically studied the formation of bumps during laser writing both experimentally and theoretically.

In the present chapter we shall round up the important results from our studies and present detailed discussions on the results. We organize the chapter as follows. In the first part, we present results of forming circular bumps as a by-production of rather conventional laser writing process for the purpose of data storage on $Ag_8In_{14}Sb_{55}Te_{23}$ chalcogenide phase change films. In this part, the detailed process of writing and erasing will be described, and

the experimental and theoretical characterizations of the bumps are demonstrated. In the second part, we expand our work to intentionally form micro patterns on multilayer ZnS-SiO_2/AgO_x/ZnS-SiO_2 thin films by laser direct writing technology. We shall conclude the work in the end of the chapter.

2. Laser pulse induced bumps in chalcogenide phase change films

Chalcogenide phase change thin films are widely used as optical and electric data storage media. The recording is based on the phase change between the crystalline and amorphous states (Kolobov et al., 2004; Kalb et al., 2004; Welnic et al., 2006; Wuttig & Steimer, 2007). In the writing process, a small volume in the thin film is locally and rapidly heated to above the melting point and successively quenched into the amorphous phase. In the erasing process, the material undergoes a relatively long heating to reach a temperature above the glass transition but yet below the melting point, which brings the material back to the crystalline phase. The heat source for the phase change is usually from laser pulses in optical data storage, or electric current pulses in electric data storage. In the present work we shall selectively concentrate on the optical storage.

In the process of amorphization, i.e., the laser writing process, the material experiences a volume change due to the stronger thermal expansion in the melting state than in the crystalline state, as well as the density difference between the two states. Therefore, the amorphous recording marks are actually physically deformed as circular bumps because the amorphous recording marks inherit the volume in the melting state after a fast cooling stage. Subsequently, the bumps may cause further deformation in other thin layers stacked underneath as in the cases of optical information memory in optical storage and the electrode in electric storage. While slight deformation in the writing process is inevitable, significant bumps are harmful for the storage media as they affect dramatically the size of the marks, which eventually reduces the recording density of the media, and shorten the durability of the device. In extreme cases the bumps may grow so big that a hole is formed at the apex of the bump. Therefore, to quantitatively describe the bump formation is of great interest for storage applications.

We have established a theoretical model for the formation process, where the geometric characters of the formed bumps can be analytically and quantitatively evaluated from various parameters involved in the formation. Simulations based on the analytic solution are carried out taking $Ag_8In_{14}Sb_{55}Te_{23}$ as an example (Wei et al., 2008; Dun et al., 2010). The results are verified with experimental observations of the bumps.

2.1 Theory

Let us start by describing the amorphization process schematically in the volume-temperature diagram as shown in Fig. 1, where the principal paths for the phase changes are depicted. Initially, the chalcogenide thin film is considered in the crystalline state represented by point *a*; a laser or current pulse of nanosecond duration heats the material up to the melting state, which is represented by point *b*. Subsequently, the material is cooled quickly with a high rate exceeding $10^7\ C/s$ to the room temperature to form the final amorphous mark. During the quenching stage, the material structure does not have sufficient time to rearrange itself and remains in the equilibrium state, and thus inherits the structure and volume at the melting state. Therefore, the volume has an increase ΔV, and

the mark appears as a bump. If the laser or current pulse injects energy higher than the ablated threshold corresponding to the vaporization temperature, the heating temperature reaches point *d*, and the material is then rapidly cooled to the room temperature, which is represented by point *e*; an ablated hole can be formed at the top of the bump.

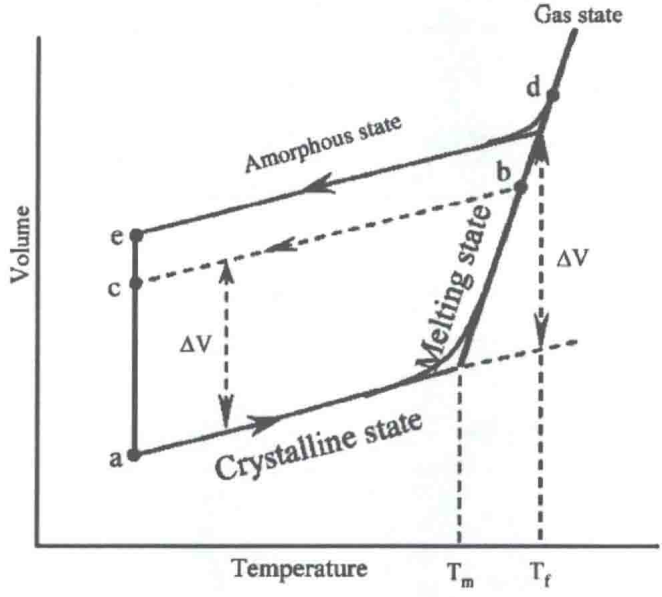

Fig. 1. Volume-temperature diagram of chalcogenide films. The film is heated by laser from point *a* to point *b* and returns to point *d*, or to point *c* and returns to point *e* after faster cooling.

The geometric characters of the bump are graphed in Fig. 2, where cross-sections of the circular bump are schematically shown respectively for the case of a bump and the case of a bump with a hole on its top. It is worth noting that, in general, the volume thermal expansion coefficient for chalcogenide thin films has two different constant values in the crystalline and melting states, respectively. In our analysis, there is assumed a Gaussian intensity profile for the incident laser pulse, and volume changes occur only in the region irradiated by the laser pulse, as shown in Fig. 2(a). If the laser pulse energy exceeds the ablated threshold, a hole is to be formed at the top of the bump, which is shown in Fig. 2(b). Mathematically, for the fast heating and amorphization process, the net volume increase can be written as $\Delta h = (\beta_m - \beta_c) \cdot V_0 \cdot (T_{surf} - T_m)$, where β_m and β_c are the volume thermal expansion coefficients in the crystalline and melting states, respectively. V_0 is the irradiated region volume. T_{surf} is the material surface temperature heated by laser pulse and T_m is the temperature corresponding to the melting point. Since the irradiated region is axially symmetric due to the Gaussian laser beam intensity profile, the bump height can be expressed as

$$\Delta h(r) = (\beta_m - \beta_c) \cdot h_0(r) \cdot (T_{surf} - T_m) \tag{1}$$

where r is the radial coordinate, and $h_0(r)$ is the height of the irradiated region.

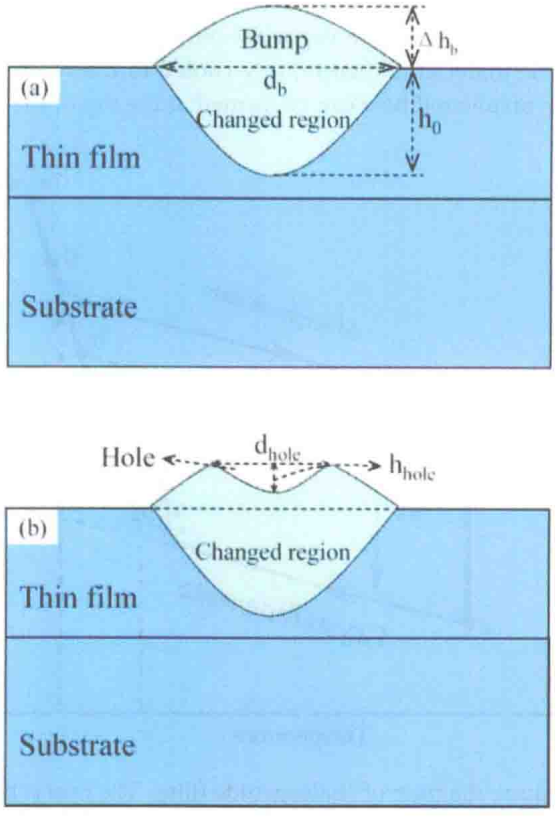

Fig. 2. Bump formation schematics: (a) bump and (b) hole on the top of bump.

Furthermore, the absorbed energy per unit volume and per unit time can be calculated by

$$g(r,z) = \alpha(1-R)\frac{2P}{\pi w^2}\exp(-\frac{2r^2}{w^2})\exp(-\alpha z) \tag{2}$$

where α is the absorption coefficient, R is the reflectivity of the material, P is the laser power, w is the laser beam radius at the $1/e^2$ of the peak intensity, and z is in the depth direction from the sample surface. In Eq. (2) the quantity $\alpha(1-R)$ is the absorbed part of the transmitted light, which decays exponentially $\exp(-\alpha z)$ along the z direction and spreads as a Gaussian function $\exp\left(-2r^2/w^2\right)$ in the r direction.
Generally for data storage, the width of the laser pulse is in the range from nanosecond to millisecond. Within this range, the temperature distribution in the irradiated region can be expressed as

$$T(r,z) = \frac{g(r,z)\tau}{\rho C_p} \tag{3}$$

where ρ is the density, C_p is the heat capacity of the material, and τ is the laser pulse width. According to (Shiu et al., 1999), the bump height $\Delta h(r)$ can be calculated, within the

temperature interval $T_m < T(r,0) < T_f$, where T_f is the temperature corresponding to the vaporization point above which the material will be ablated, by

$$\Delta h(r) = \frac{\beta_m - \beta_c}{\alpha}[T(r,0) - T_m]\ln\left[\frac{T(r,0)}{T_m}\right] \tag{4}$$

and the bump diameter d_p can be calculated by setting $T(r,0) = T_m$ and $r = d_p/2$ in Eq. (3) with

$$d_p = \sqrt{2}w\sqrt{\ln\left[F_0\frac{\alpha(1-R)}{\rho C_p}\right]\frac{1}{T_m}} \tag{5}$$

where $F_0 = 2P\tau/\pi w^2$. Similar to the derivation of bump diameter, if the laser pulse energy exceeds the ablated threshold, an ablated hole is formed when $T(r,0) > T_f$ and the hole diameter in the bump d_{hole} can be calculated as

$$d_{hole} = \sqrt{2}w\sqrt{\ln\left[F_0\frac{\alpha(1-R)}{\rho C_p}\right]\frac{1}{T_f}} \tag{6}$$

It should be noted that in our analytical model, the thermo-physical parameters of material are assumed independent from temperature.

2.2 Experimental observations

Before presenting results of simulation based on the above developed formalism, let us show some experimental observations of the bumps. The experimental results provided useful and meaningful values for choosing the parameters involved in the theoretical simulations. In the experiments, $Ag_8In_{14}Sb_{55}Te_{23}$ thin films were directly deposited on a glass substrate by dc-magnetron sputtering of an $Ag_8In_{14}Sb_{55}Te_{23}$target. The light source is a semiconductor laser of wavelength $\lambda = 650nm$, and the laser beam is modulated to yield a $50ns$ laser pulse. The laser beam is focused onto the $Ag_8In_{14}Sb_{55}Te_{23}$ thin film, and the light spot diameter is about $2\mu m$. In order to form bumps with different sizes, various laser power levels were adapted. Some of the experimental results are presented in Figs. 3–5.

Fig. 3(a) shows some bumps obtained with laser power $3.8mW$. The inset in Fig. 3(a) is an enlarged image of one bump. The bump diameter is about $0.9-1.0\mu m$. In order to further analyze the bump morphology, an atomic force microscope (AFM) was used to scale the bump. The results are shown in Fig. 3(b), where the top-left inset shows the same bumps as in Fig. 3(a), and the top-right inset is the cross-section profile of the bump. One notes that the bump height is about $60-70nm$, and the diameter is about $1\mu m$. With the increase of laser power, a round hole in the bump is formed, as shown in Fig. 4, where the laser powers are 3.85, 3.90, and 4.0 mW, respectively. The corresponding bumps are shown from left to right in Fig. 4.

The bumps in Fig. 5(a) were produced at laser power level 4.0 mW. In Fig. 5(a) the left-bottom inset is an enlarged bump image. It is found that holes are formed in the central region of the bumps. Fig. 5(b) presents the AFM analysis, where the top-right inset is the three-dimensional bump image. It can be seen that the bump diameter is about $1\mu m$, and the size of the hole is about $250-300nm$.

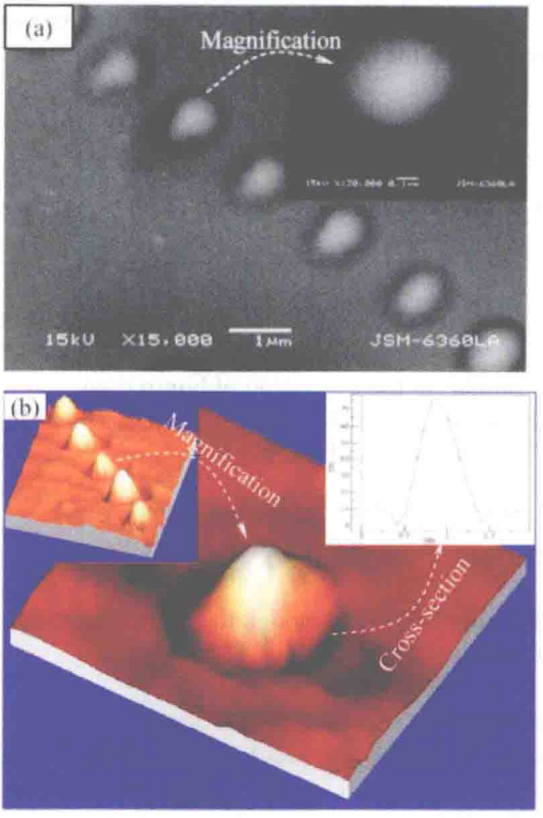

Fig. 3. Bumps formed at laser power $3.8mW$: (a) SEM analysis and (b) AFM analysis.

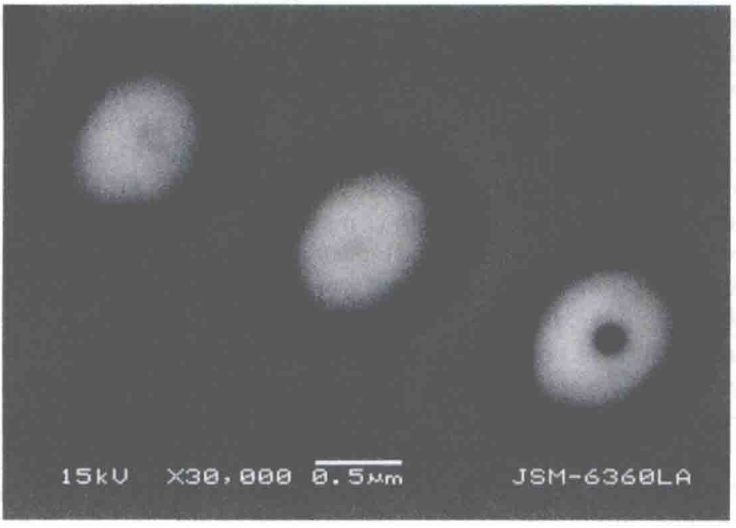

Fig. 4. SEM analysis for bumps formed at laser power of 3.85 , 3.90 and $4.0mW$.